Non-Darcy Forchheimer Effect on Boundary Layer Stagnation Point Flow of Fe₃O₄-Ethylene Glycol/Engine Oil Over Non-Linearly Expanding Sheet

Arijit Mandal,

Ph. D Scholar in Dr. A. P. J. Abdul Kalam University, Indore, Madhya Pradesh - 452016 E-mail: arijitmandal.mld@gmail.com

Dr. Annapurna Ramakrishna Sinde,

Department of Mathematics, Dr. A. P. J. Abdul Kalam University, Indore, Madhya Pradesh - 452016 E-mail: jayabhandari15@gmail.com

Dr. Md Tausif Sk,

Department of Mathematics, Acharya B.N. Seal College, Cooch Behar - 736101, West Bengal, India E-mail: tausifdropbox@gmail.com

Article Info
Page Number: 13293 – 13298
Publication Issue:
Vol 71 No. 4 (2022)

Abstract: A logical and mathematical enquiry has been executed to compare the mathematical information and graphical figures of two unique sorts of nanofluid limit layer stream in a non-Darcy permeable medium with Fe3O4.nanoparticle in the liquid. The ongoing surface is persistently extended under a proper regulation and the base fluids are ethylene glycol and motor oil. A numerical model of the stream has been organized and in the wake of redesigning the non-straight fractional differential conditions into an arrangement of Tribute, it has been tackled both systematically by Differential Change Strategy (DTM) in participation with Pade Approximant and mathematically by Runge-Kutta fourth request shooting procedure. The total of the relations between different stream boundaries with the skin grating and the intensity move pace of two unique liquids have been checked by connection coefficients and the effect of the connection has been confirmed utilizing Fisher's t-Test. One of the most fascinating decisions of the advancement study is that the pace of intensity move rate in the Fe3O4-motor oil nanofluid is just about 83-88% higher than that of Fe3O4ethylene glycol nanofluid. Likewise, the connection between different relevant boundaries with the Nusselt number and the skin rubbing coefficient are profoundly huge and they can be directed by our necessity by controlling these boundaries of the stream.

Article History
Article Received: 25 October
2022

Revised: 30 November 2022 Accepted: 15 December 2022 **Keywords and phrases:** Nanofluid; Thermal Radiation; DTM; Pade Approximant; Correlation Coefficient; Fisher's t-test.

INTRODUCTION:

The investigation of liquid stream, wall shear pressure and intensity move rate through permeable medium is a significant need of the present current progress. There are many fields like mechanical, common and synthetic designing require the broad review and stream examination in permeable

medium to deliver some designing devices productive to humankind. A few ecological reviews like petrol designing, ground water hydrology, water asset designing and so on are there, where permeable medium is normally found. In this way to expand the development of petroleum derivative or ground water, world requires a significant aftermaths and plan to support the creation and limit the wastage of them. The investigation of permeable medium is fundamental for methane recuperation from ground repositories by consistent depressurization and CO2 sequestration. Additionally, as of late it is fundamental in water filtration framework (RO), atomic garbage removal, energy unit layer with electrochemistry, biomedical medical procedures. Prior Minkowycz and Cheng [1] examined the free convective stream in a permeable medium in an upward plate. Hong et al. [2] examined the Darcy impact in a non-uniform permeable medium over an upward plate. As indicated by Darcy regulation the tension inclination is directly corresponding to the speed of the stream, which was laid out tentatively by a one layered water move through stuffed sands at low speed. However, the law is restricted in low-speed stream and low Reynolds' number. In this way different endeavors were made by numerous researchers to vanish the limit of the Darcy's regulation. In 1901, an Austrian architect P. Forchheimer made an improvement in Darcy's regulation by adding a second request speed term to address the minute inertial impact because of the communication among solids and liquids in the stream and presented non-Darcy impact in the stream. Numerous scientists like Lai et al. [3] examined non-Darcy stream in soaked permeable medium. Kandasamy et al. [4] noticed the presentation non-Darcy MHD nanofluid stream over a permeable wedge. As of late Lebeau and Konrad [5] observed that Darcy regulation is lacking to portray the connection between the shallow motion and slope in rock fill materials. In this way, they use non-Darcy impact to outline the radiative intensity move trademark and warm reaction of the rail line bank.

MHD stream over constantly extensible surface is huge in numerous modern creations like polymer industry, substance industry, creation of optical filaments and so on. Crane [6] had dissected first the liquid stream over an extending sheet. Then Chen and Scorch [7] noticed the way of behaving of intensity move pace of the liquid over an extending sheet. Stagnation point stream over a warmed extending permeable sheet was examined by Layeket al. [8]. Ishaket al. [9] concentrated on MHD limit layer stream because of extensible surface. Weidman et. al. [10] summed up crafted by Crane [6] over an extending sheet by presenting erratic speeds. As of late Ahmed et al. [11] tackled mathematical arrangements of MHD nanofluid stream overa bi-directional dramatically extending sheet. Recently, Sk et al. [12] broke down mathematically the impact of outside attractive field over a MHD nanofluid current incited over a non-straightly extending sheet and tracked down a wonderful impact of attractive field on relevant boundaries of the stream.

Pretty much every numerical demonstrating requires straight or non-direct differential conditions to explain the relations between its relevant boundaries and its factors. In this way, to tackle those differential conditions precisely, around or mathematically specialists look for a useful asset to limit the computational work and expand the mark of union and exactness. Different techniques like HAM, VIM, VPM, ADM, HPM and FDM are there to tackle straight and non-direct differential conditions, however every one of them have a few restrictions. They require estimations a considerable amount. Running against the norm Differential Change Technique is such strategy that requires less calculations and can give profoundly exact rough arrangements like others. In the year 1986 Chinese Researcher J. K. Zhou [13] first presented DTM before the world to research IVP connected with the investigation of Circuits. Later two layered DTM was presented by Jang et al. [14]. A relative report among DTM and ADM was dissected by Hassan [15] during the investigation of Tumult. Then, at that point, KdV and mKdV conditions were addressed utilizing DTM by Kangalgil and Ayaz [16]. Pekeret al. [17] endeavored to tackle Blassius conditions with unbounded limit conditions utilizing DTM and Pade approximant. In that concentrate on the presumed that the outcomes acquired by ADM, DTM with Pade approximant, VIM were in colossal understanding, yet calculations were especially diminished. As of late Kundu et al. [18] inspected the warm way of behaving of wet balances with remarkable profiles utilizing DTM.

Convective intensity move through nanoparticles is a famous area of exploration now days. Nanofluid is a high-level sort of material containing suspension of strong particles called nanoparticles in customary intensity move liquids (H2O, oil and ethylene glycol). It has acquired a lot of significance of the scientists because of improved warm conductivity and convective intensity move coefficient.

Attractive or ferrofluid are extraordinary sort of nanofluids which are suspensions of attractive nanoparticles (magnetite, hematite, cobalt ferrite or some other compound containing iron) in regular base liquid. Attractive nanofluid is a remarkable material that has both the fluid and attractive properties. Without any attractive field these liquids act as typical nanofluids. Such liquids have been found to have a few entrancing applications, for example, magneto-optical frequency channel, optical modulators, nonlinear optical materials, tunable optical fiber channel, optical grinding, optical switches and so on. Ferrofluid are blended liquids with profoundly thought colloid suspensions of fine attractive particles in non-leading transporter liquids. Magneto nanofluids are helpful to direct the particles up the circulatory system to a cancer with magnets. This is because of the way that the attractive nanoparticles are respected more glue to growth cells than non-harmful cells. Such particles assimilate more power than miniature particles in substituting current attractive fields mediocre in people for example for disease treatment. Various applications including attractive nanofluids incorporate medication conveyance, hyperthermia, contrast improvement in attractive reverberation imaging and attractive cell partition. Persuaded by all the previously mentioned realities, different researchers and specialists are participated in the conversation of streams of ferrofluid by means of various viewpoints. Selimefendigil et al. [19] concentrated on the alternating chamber impacts in constrained convection of ferrofluid over a regressive confronting step. Nanjundappa et al. [20] portrayed the ferroconvection in ferrofluid soaked permeable layer warmed from beneath and cooled from above with consistent intensity transition subject to attractive field subordinate (MFD) thickness. Sheikholeslami et al. [21] talked about the impact of outside attractive field with free convection of ferrofluid present in hole warmed from underneath. Titus and Abraham [22] broke down the ferrofluid stream and intensity move over an extending sheet with radiation. Sheikholeslami and Ganji [23] concentrated on the MHD and ferrohydrodynamics consequences for ferrofluid stream and convective intensity move. Smash and Sharma [24] introduced the impact of MFD consistency and porosity with turning plate on spinning ferrofluid. Shehzad et al. [25] analyzed thermally radiative three-layered progression of Jeffrey nanofluid with interior intensity age and attractive field. Hayat et al. [26] examined effect of homogeneous-heterogeneous responses in MHD stream of nanofluid subject to second request slip speed. Heat move in MHD blended convection stream of a ferrofluid along an upward channel has been explored by Gul et al [27]. Hayat et al. [28] examined impacts of homogeneous-heterogeneous responses in progression of magnetite-Fe3O4 nanoparticles by a pivoting plate.

Utilization of hydrocarbon fills as cooling specialist in rocket motors and as refrigerant in scramjet motors are especially famous for change in warm properties at supercritical strain point. Its particular intensity limit differs with temperature and achieves its greatest worth at a specific temperature, which is called pseudo-basic temperature at that basic strain. Hydrocarbons have more muddled atomic construction than water and CO2. That is the reason hydrocarbons like motor oil have more proficiency to move heat. X. Li et al. [29] consider the China No. 3 avionics motor oil violent stream at supercritical strain and concentrated on the intensity move capacity of the liquid. Agarwal et al. [30] explored assuming the intensity move limit of lamp fuel can be improved at room warming. For that reason, they added Al2O3 nanoparticle to the lamp oil and saw that intensity move limit expanded by practically 22% and consistency expanded by 10%. Later they [31] contemplated graphene-lamp oil nanofluid. They laid out that the warm conductivity of the lamp fuel graphene compasses to its pinnacle esteem at a specific surface area of 750 m2/g and 2% nanoparticle focus. Khan et al. [32] applied VPM to concentrate on the press stream of Cu-water and Cu-lamp fuel nanofluids between two equal plates under the thought of speed dispersal and slip condition at the limit layer.

In the current examination we have thought about permeable medium as the stream media. Then for the impediment of Darcy's regulation we have added Forchheimer number to broaden its materialness. We have utilized Fe3O4 nanoparticle in two unique kinds of base liquid like ethylene glycol and motor oil. Additionally, the outer layer of the stream is persistently broadened. The administering PDE is changed to Tribute and utilizing DTM with Pade approximant an estimated scientific arrangement is gotten and contrasted the outcome and mathematical outcome tracked down utilizing Runge-Kutta Technique for fourth request. Then a rundown of connection coefficients between relevant boundaries and the amounts of actual interests has determined to gauge how much connection between them. The legitimacy of the connection coefficient is researched by Fisher's t-test. The speed and temperature profile of the stream for both the base liquids are portrayed and thought about through

the diagrams and graphs. Finally, we examined the discoveries of the current concentrate in a systematic design.

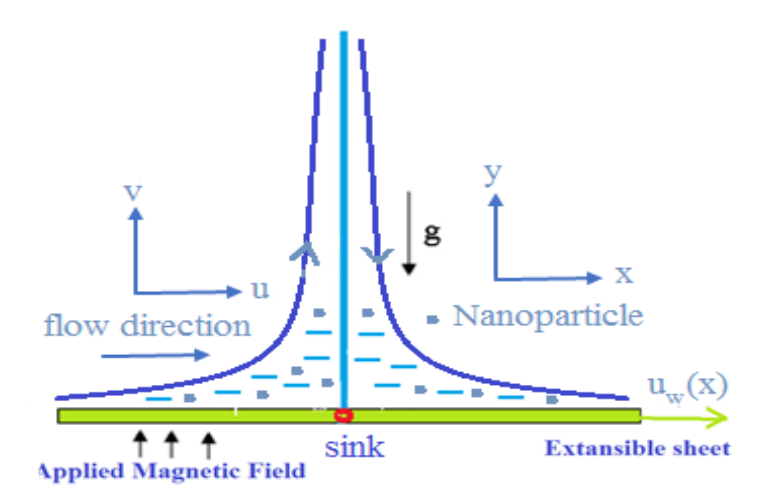


FIGURE 1: PHYSICAL MODEL OF THE FLOW

FLOW ANALYSIS:

The intensity move character is broke down of two layered limit layer nanofluid stream over a constantly extensible sheet in a soaked permeable media with no-slip condition in the limit. An outside heat radiation applied to the expanding surface of the stream and an outer cross over attractive field

$$B(x) = B_0 \left(\frac{x_0}{|x|}\right)^{\frac{n+1}{2}}$$
, have been utilized to the typical bearing of the stream. Likewise, we consider the

temperature at the wall is given by
$$T_w = T_\infty + T_0 \left(\frac{x_0}{|x|}\right)^m$$
, where T_∞ is the temperature of the liquid at a

long way from the emanated wall, T_0 is the temperature size of the stream. The inward attractive field is thought to be too little to possibly be overlooked as the attractive Reynolds' number estimated to be extremely low. The outer layer of the stream is set at y=0 and the liquid is streaming because of the extending of the surface over the locale y>0. The expansion of the wall is administered by the law

$$u_w = U_0 \left(\frac{x_0}{|x|}\right)^n$$
, where U_0 is considered as trademark worth of the speed of the stream, is the speed

power file. It is qualified to tell that there is a sink in the wall at (0,0). So speed of the stream at (0,0) breaks up in a sink. We additionally accept that no voltage has been applied and the Fe3O4 nanoparticle and the base liquids, say ethylene glycol and motor oil are together as one. The actual circumstance of the stream is portrayed in Fig-1.

Under all the above thought the administering conditions of movement of the stream is as per the following:

$$\frac{\partial u}{\partial x} + \frac{\partial u}{\partial y} = 0 \tag{1}$$

$$u\frac{\partial u}{\partial x} + v\frac{\partial u}{\partial y} = v_{nf}\frac{\partial^2 u}{\partial y^2} - \frac{\sigma B^2 u}{\rho_{nf}} - \frac{v_{nf}u}{k} - \frac{k'}{\sqrt{k}}u^2$$
(2)

$$u\frac{\partial T}{\partial x} + v\frac{\partial T}{\partial y} = \frac{\kappa_{nf}}{\left(\rho C_p\right)_{nf}} \frac{\partial^2 T}{\partial y^2} - \frac{1}{\left(\rho C_p\right)_{nf}} \frac{\partial q_r}{\partial y}$$
(3)

Here u and v are the speed parts, $v = \frac{\mu}{\rho}$ is kinematic consistency, σ is the electrical

conductivity, ρ is the thickness, $k = k_0 \left(\frac{x_0}{|x|}\right)^{-(n+1)}$ is the porosity of the permeable media presented by

Darcy which portrays the drag of the stream, $k' = k_0' \left(\frac{x_0}{|x|}\right)^{-\frac{n-1}{2}}$ addresses inertial of the stream presented

by Forchheimer which goes from 0.05 to not entirely set in stone through different trials in permeable media, K characterizes warm conductivity, C_p represents explicit intensity at perpetual tension,

$$q_r = -\frac{4\sigma^*}{3k^*} \frac{\partial T^4}{\partial y}$$
 characterizes heat radiation motion for the wall, σ^* characterizes the consistent of

Stefan Boltzmann and k^* characterizes the steady of mean retention of warm radiation by the liquids, ()_{nf} represents different actual properties of the nanofluid.

The related limit states of the stream for better representation of the ideal numerical demonstrating and state of being are given underneath:

$$u = u_w(x), v = 0, T = T_w(x) \quad \text{at y=0}$$

$$u = 0 \text{ and } T \to T_\infty \quad \text{as y} \to \infty$$

$$u \to 0 \text{ and } T \to T_\infty \quad \text{as x} \to -\infty$$

$$(4)$$

The declaration of different actual proportions of nanofluid, for example, thickness, consistency, warm conductivity and explicit intensity limit are communicated as resulting:

$$\rho_{nf} = (1 - \phi) \rho_f + \phi \rho_n$$

$$\mu_{nf} = \frac{\mu_f}{(1 - \phi)^{2.5}}$$

$$\kappa_{nf} = \frac{\left(\kappa_n + 2\kappa_f\right) - 2\phi\left(\kappa_n - \kappa_f\right)}{\left(\kappa_n + 2\kappa_f\right) + \phi\left(\kappa_n - \kappa_f\right)} \kappa_f$$

$$\left(\rho C_p\right)_{nf} = (1 - \phi) \left(\rho C_p\right)_f + \phi \left(\rho C_p\right)_n$$
(5)

Here ϕ is the nanoparticle volume portion present in the base liquid, ()_n stands to address upsides of nanoparticles for example Fe3O4, ()_f represents upsides of base liquids in here its either ethylene glycol or motor oil. The thermo actual assets of the liquids and nanoparticle are uncovered in table-1.

TABLE 1 THERMO PHYSICAL POSSESSIONS OF ETHYLENE GLYCOL, ENGINE OIL AND FE₃O₄ NANOPARTICLE [32]:

	P (Kg/m ³)	$C_p(J/kg.K)$	K (W/m.K)	
Ethylene glycol	1115	2430	0.253	
Engine oil	884	1910	0.144	

Fe ₃ O ₄	5180	670	6
--------------------------------	------	-----	---

Under every one of the above guesses and redesigns the overseeing condition of the current stream is currently at non-straight structure, which is very burdensome to tackle. So to ease and work on the retributions, we familiarize with a bunch of similitude changes so the PDE type of overseeing conditions can be changed to an arrangement of common differential conditions alongside the limit conditions. The changes are

$$\eta = y \left(\frac{u_w}{2v_f |x|} \right)^{\frac{1}{2}}, f(\eta) = \frac{\psi}{\left(2v_f u_w |x| \right)^{\frac{1}{2}}}, \theta(\eta) = \frac{T - T_{\infty}}{T_w - T_{\infty}}$$
 (6)

Here η is closeness variable, $f(\eta)$ is non-layered stream capability, ψ is conventional stream capability declared to communicate u and v as $u = \frac{\partial \psi}{\partial y}$, $v = -\frac{\partial \psi}{\partial x}$ so condition (1) obviously fulfilled,

 $\theta(\eta)$ frames non-layered temperature of the liquid. Presently in the wake of drawing in equ.(6)in u and v, we can explain them as

$$u = u_w \frac{df}{d\eta}, v = -\left(\frac{2v_f u_w}{|x|}\right)^{\frac{1}{2}} \left(\frac{n-1}{2}f + \frac{n+1}{2}\frac{df}{d\eta}\right)$$
 (7)

Utilizing conditions (6) and (7) in conditions (2) and (3) alongside the limit conditions (4), we acquired the changed arrangement of Tribute for the present numerical model with Beginning limit condition.

$$(1-\phi)^{-2.5} \left(\frac{d^3 f}{d\eta^3} - k_1 \frac{df}{d\eta} \right) - 2M \frac{df}{d\eta} + \left(1 - \phi \left(1 - \frac{\rho_n}{\rho_f} \right) \right) \left\{ (n-1) f \frac{d^2 f}{d\eta^2} - \left(2n + k_2 \right) \left(\frac{df}{d\eta} \right)^2 \right\} = 0$$
 (8)

$$\frac{\kappa_{nf}}{\kappa_{f}} \frac{d^{2}\theta}{d\eta^{2}} + \frac{4}{3} N_{r} \frac{d}{d\eta} \left\{ \left(C_{T} + \theta \right)^{3} \frac{d\theta}{d\eta} \right\} + P_{r} \frac{\left(\rho C_{p} \right)_{nf}}{\left(\rho C_{p} \right)_{f}} \left[(n-1) f \frac{d\theta}{d\eta} - 2m\theta \frac{df}{d\eta} \right] = 0$$

$$(9)$$

The transformed boundary conditions are given by:

$$f(0) = 0, \frac{df}{d\eta}\Big|_{\eta=0} = 1, \theta(0) = 1$$

$$\frac{df}{d\eta} \to 0 \text{ and } \theta(\eta) \to 0 \text{ as } \eta \to \infty$$
(10)

Here $k_1 = \frac{2v_f}{U_0 k_0 x_0}$ defines porosity factor, $k_2 = \frac{2k_0'}{\sqrt{k_0} x_0}$ represents the constraint of inertial

consequence, $M = \frac{\sigma B_0^2 x_0}{U_0 \rho_f}$ depicts parameter of magnetism, $P_r = \frac{v_f \left(\rho C_p\right)_f}{\kappa_f}$ is Prandtl Number,

$$N_r = \frac{4\sigma^* T_{\infty}^3}{\left(\rho C_p\right)_f k^*} \text{ signifies the thermal radiation parameter, } C_T = \frac{T_{\infty}}{T_w - T_{\infty}} \text{ indicates temperature ratio}$$

which is a very tiny quantity as T_{∞} assumes to be very slight associated to $T_{w} - T_{\infty}$.

In this study the calculable amounts of the stream are skin erosion coefficient that addresses the wall shear pressure between the surface and the nanofluid, and the other is Nusselt number that characterizes the intensity move rate that moved by the nanofluid in the stream. They can be communicated as

$$C_f = \frac{2\tau_w}{\rho_f u_w^2} \quad \text{and} \quad \text{Nu} = \frac{xq_w}{\kappa_f (T_w - T_\infty)}$$
(11)

Here the shear stress τ_w and heat flux q_w at the surface of the flow can be expressed as

$$\tau_{w} = \mu_{nf} \left(\frac{\partial u}{\partial y} \right)_{y=0} \quad \text{and} \quad q_{w} = -\kappa_{nf} \left(\frac{\partial T}{\partial y} \right)_{y=0}$$
(12)

Introducing (6) and (7) in (11) and (12), we finalize the expression for local skin friction coefficient and local Nusselt number as follows:

$$C_{f}r = C_{f}\sqrt{\operatorname{Re}_{x}} = \frac{\sqrt{2}}{\left(1-\phi\right)^{2.5}} \frac{d^{2}f}{d\eta^{2}}\Big|_{\eta=0}$$

$$\operatorname{Nur} = \frac{\operatorname{Nu}}{\sqrt{\operatorname{Re}_{x}}} = -\frac{\kappa_{nf}}{\sqrt{2}\kappa_{f}} \left[1 + \frac{4}{3}N_{r}\left\{C_{T} + \theta(0)\right\}^{3}\right] \frac{d\theta}{d\eta}\Big|_{\eta=0}$$
(13)

Here $\operatorname{Re}_{x} = \frac{u_{w}|x|}{v_{f}}$ represents the reduced Reynolds's Number.

METHOD OF SOLUTION:

ANALYTIC SOLUTION USING DTM AND PADE APPROXIMANT:

If $F(\mathbf{k})$ is the one variable transformed function of $f(\mathbf{x})$ at $\mathbf{x} = \mathbf{x}_0$, then we get from DTM that

$$F(k) = \frac{1}{|k|} \frac{d^k f}{dx^k} \bigg|_{x=x_0}$$
 (14)

Also the inverse differential transform of F(k) is defined by

$$f(x) = \sum_{n=0}^{\infty} (x - x_0)^k F(k)$$

$$f(x) = \sum_{n=0}^{\infty} \frac{1}{|k|} \frac{d^k f}{dx^k} \bigg|_{x=x_0} (x-x_0)^k$$
, which is the expression of Taylor's series expansion of $f(x)$ at

$$x = x_0$$
.

After employing the above definition to the equations (8) and (9), we get $(k+1)(k+2)(k+3)F(k+3)-(2ABM+k_1)(k+1)F(k+1)$

$$+ABC\sum_{k=0}^{k} (k-r+1)F(r)F(k-r+1) - ABD\sum_{k=0}^{k} (k-r+1)(r+1)F(r+1)F(k-r+1) = 0$$
(15)

$$(k+1)(k+2)\Theta(k+2) + C(k+1)\sum_{r=0}^{k+1}\sum_{r_1=0}^{r}\sum_{r_2=0}^{r_1}(k-r+2)\Theta(r_2)\Theta(r_1-r_2)\Theta(r-r_1)\Theta(k-r+2)$$

$$+(n-1)E\sum_{r=0}^{k}(r+1)\Theta(r+1)F(k-r) - 2mE\sum_{r=0}^{k}(r+1)F(r+1)\Theta(k-r) = 0$$
(16)

Here F(k) and $\Theta(k)$ are the differential transforms at $\eta = 0$ of $f(\eta)$ and $\theta(\eta)$ respectively, also

$$A = (1 - \phi)^{2.5}, B = 1 - \phi \left(1 - \frac{\rho_n}{\rho_f}\right), C = \frac{4}{3} \frac{\kappa_f}{\kappa_{nf}} N_r, D = (2n + k_2), E = P_r \frac{\kappa_f}{\kappa_{nf}} \frac{(\rho C_p)_{nf}}{(\rho C_p)_f}$$

and the initial values are obtained form (10) as,

$$F(0) = 0, F(1) = 1, \Theta(0) = 1$$

Also assume that $\frac{d^2 f}{d\eta^2}\Big|_{\eta=0} = \alpha$ and $\frac{d\theta}{d\eta}\Big|_{\eta=0} = \beta$ then $F(2) = \frac{\alpha}{2}$, $\Theta(1) = \beta$. Now if we apply the above

initial conditions in (15) we obtain,

$$F(3) = \frac{1}{2} (k_1 + 2ABM + 2ABD)$$

$$F(4) = \frac{1}{4} \left\{ \left(k_1 + 2ABM + 2ABD \right) \alpha - ABC \right\}$$

$$F(5) = \frac{1}{|5|} \left\{ \left(k_1 + 2ABM + 2ABD \right)^2 - \frac{3}{2} \alpha ABC + 2\alpha^2 ABD \right\}$$

$$F(6) = \frac{1}{6} \left[\frac{-12ABC(k_1 + 2ABM + 2ABD) + (k_1 + 2ABM + 2ABD)^2 + 6ABD(k_1 + 2ABM + 2ABD)}{(k_1 + 2ABM + 2ABD)^2 + 6ABD(k_1 + 2ABM + 2ABD)} \alpha + 2\alpha^2 ABC \right]$$

and so on.

Similarly from (16) we get,

$$\Theta(2) = \frac{2mE - 3C(C_T + 1)^2 \beta^2}{2!(C(C_T + 1)^3 + 1)}$$

$$\Theta(3) = \frac{1}{3!} \left(C(C_T + 1)^3 + 1 \right)^{-2} \left[\left(C(C_T + 1)^3 + 1 \right) \left\{ mE(\alpha + 2\beta) - m\beta(n-1) - 6C(C_T + 1)\beta^3 \right\} \right] + 9C(C_T + 1)^2 \beta \left\{ 2mE - 3C(C_T + 1)^2 \beta^2 \right\}$$

and so on.

In order to find the value of α and β we undertake that $\phi = 0, k_1 = 0, M = 0, n = \frac{3}{2}, k_2 = 0.3, N_R = 0, P_r = 1, m = 0, C_T = 0$ and using [2/2] Pade

Approximant[17]to approximate the functions $\frac{df}{d\eta}$ and $\theta(\eta)$ and applying the boundary conditions

 $\lim_{\eta \to \infty} \frac{df}{d\eta} = 0 \text{ and } \lim_{\eta \to \infty} \theta(\eta) = 0 \text{ we get, } \alpha = 0.5773502693 \text{ which show excellent agreement with the work of Peker et al. [17] and we found } \beta = 0.4237768.$

NUMERICAL SOLUTION BY RUNGE- KUTTA 4TH ORDER METHOD:

After doing all those analytic work, we are looking for numerical solution of the transformed non-linear ordinary differential equations in (12), (13) along with the boundary conditions (14). For this

purpose we consider that
$$f = f_1$$
, $\frac{df}{d\eta} = f_2$, $\frac{d^2 f}{d\eta^2} = f_3$, $\theta = f_4$, $\frac{d\theta}{d\eta} = f_5$ then the reduced set of ODE is

Subsequent to doing that large number of logical work, we are searching for mathematical arrangement of the changed non-straight standard differential conditions in (12), (13) alongside the

limit conditions (14). For this reason we consider that $f = f_1$, $\frac{df}{d\eta} = f_2$, $\frac{d^2f}{d\eta^2} = f_3$, $\theta = f_4$, $\frac{d\theta}{d\eta} = f_5$

then the diminished arrangement of Tribute is

$$\frac{df_{1}}{d\eta} = f_{2}$$

$$\frac{df_{2}}{d\eta} = f_{3}$$

$$\frac{df_{3}}{d\eta} = (k_{1} + 2M) f_{2} - (1 - \phi)^{2.5} \left\{ 1 - \phi \left(1 - \frac{\rho_{n}}{\rho_{f}} \right) \right\} \left\{ (n - 1) f_{1} f_{3} + (2n + k_{2}) (f_{2})^{2} \right\}$$

$$\frac{df_{4}}{d\eta} = f_{5}$$

$$\frac{df_{5}}{d\eta} = \left[\frac{\kappa_{nf}}{\kappa_{f}} + \frac{4}{3} N_{r} (f_{4} + C_{T})^{3} \right]^{-1} \left[P_{r} \frac{(\rho C_{p})_{nf}}{(\rho C_{p})_{f}} \left\{ 2m f_{2} f_{4} - (n - 1) f_{1} f_{5} \right\} + 4N_{r} (f_{4} + C_{T})^{2} f_{5}^{2} \right]$$

and the reduced boundary conditions are

$$f_1(0) = 0, f_2(0) = 1, f_4(0) = 1$$

Since above diminished an arrangement of Tribute has five questions, so we expected five starting qualities in the limit condition to track down its answer. For that object how about we expect to be that $f_3(0) = \delta_3$, $f_5(0) = \delta_5$. Additionally it is given in the limit condition that $f_2(\infty) = 0$, $f_4(\infty) = 0$. Presently the decreased Tribute with the limit is tackled mathematically focusing on the enhancing the arrangement with δ_3 , δ_5 .

Taking on the Runge-Kutta fourth request strategy with shooting method we settle the above diminished arrangement of Tribute with the assistance of the code of Maple 17. In this strategy there are two sorts of blunder, adjust mistake and Truncation blunder, involved. The explanation of taking on this technique is that, it limits the adjust mistake and the calculations are extremely famous in fourth request strategies. The internal emphasis happens until the combination of the arrangement with an intermingling model of 10^{-6} in all cases holds.

CODE VERIFICATION:

To check the legitimacy and proficiency of the mathematical result acquired by RK-4 technique and scientific arrangement created by DTM strategy with Pade approximant, we analyze the determined upsides of $\theta'(0)$ for different upsides of porosity boundary k_1 in table-2. We found in this cycle that the mathematical and logical arrangements are in fantastic understanding and that is approved our answers and conversations of the numerical model of the current paper.

TABLE 2: COMPARISON OF VARIOUS VALUES OF $\theta'(0)$ FOR DIFFERENT VALUES OF POROSITY PARAMETER (k_1) :

k_1	DTM with Pad	e approximant	Runge-Kutta method of 4 th order			
	Fe ₃ O ₄ -ethylene glycol			Fe ₃ O ₄ -engine oil		
0.0	-2.68774	-5.16766	-2.687743146	-5.167665042		
0.1	-2.66635	-5.14467	-2.666347947	-5.144674928		
0.2	.2 -2.64658 -5.12388		-2.646580978	-5.123879989		

0.3	-2.62819	-5.10489	-2.628200774	-5.10488292
0.4	-2.614348	-5.09076	-2.614348316	-5.090756885

STATISTICAL ANALYSIS:

EXPLORATION OF CORRELATION COEFFICIENT:

In this paper we check the strength and pattern of the relationship among the various pertinent variables of the stream with the Skin grinding coefficient and Nusselt number involving connection coefficient as it is a compelling apparatus to figure the soundness of the affiliation. Mathematically we get a bunch of values for wall erosion coefficient and Nusselt Number and interaction the connection coefficients utilizing those information expecting that the boundaries and actual limits are ordinarily dispersed just to get a reasonable mindfulness about the relationship among them. Here in table-3we clarify the planned relationship coefficients.

TABLE 3: CORRELATION COEFFICIENTS AMONGST NUMEROUS FACTORS OF THE FLOW AND PHYSICAL CAPACITIES:

LOW AND INTERCAL CANACITES.								
Correlation Coefficient	C_{j}	e r	Nu	ır				
	Ethylene glycol	Engine oil	Ethylene glycol	Engine oil				
k_1	0.998916	0.998916	-0.999629	-0.999338				
k_2	-0.998378	-0.998378	0.998261	0.998316				
n	0.997868	0.997868	-0.997192	-0.995432				
φ	0.998188	0.998188	-0.999921	-0.999945				

At the point when the appraisal of relationship coefficient is negative it estimates that the factors are adversely interrelated i.e., when the worth of autonomous variable raises to higher worth the free factors diminishes. Opposite influence saw if there should arise an occurrence of decidedly corresponded factors. The nearer the worth of connection is to ± 1 , the relationship develop into stronger. Here it is detected that from the table-3that skin grinding coefficients for both ethylene glycol and motor oil are adversely corresponded with Forchheimer number and decidedly related with porosity boundary, speed power file and nanoparticle volume division. Nusselt numbers for both the ethylene glycol and motor oil are exceptionally emphatically related with Forchheimer number, speed power file and nanoparticle volume portion and adversely connected with porosity boundary, speed power record of the wall and nanoparticle volume division. Here we think about the size of the skin grinding coefficient simply regardless to the bearing of the worth.

TESTING OF SIGNIFICANCE BY FISHER'S t- TEST:

At this point creators have practiced the Fisher's t-test to evaluate the degree of meaning of connection coefficients. So, for this reason we draw in the help of Understudy's t dissemination with 3 level of opportunity. Fisher took on the invalid speculation $H_0: \rho = 0$ the populace relationship coefficient isn't

critical. The measurement:
$$t = \frac{r\sqrt{n-2}}{\sqrt{1-r^2}}$$
, where $r =$ connection coefficient and $n = 5$, follows

Understudy's t-dissemination with 3 level of opportunity. In the event that the extent of 't' ended up being past the arranged worth, Fisher understood that 't' is critical and we overruled the invalid speculation. The various upsides of 't' is recorded in table-4 and the standard classified worth of 't' is given in table-5 level of opportunity and level of importance.

TABLE 4 TABULATED MAGNITUDE OF 't' FOR DIFFERENT VALUES OF 'r':

$t = \frac{r\sqrt{n-2}}{\sqrt{n-2}}$	$C_f r$		Nur		
$t - \frac{1}{\sqrt{1-r^2}}$	ethylene glycol	engine oil	ethylene glycol	engine oil	
k_1	37.1630269	37.163027	63.6289	47.5799	
k_2	30.3716348	30.371635	29.3339	29.8091	
n	26.4823626	26.482363	23.0556	18.0549	
ϕ	28.7313873	28.732651	136.922	122.465	

TABLE 5 SIGNIFICANT VALUES OF STUDENT'S t-DISTRIBUTIONS:

Deg. Of	Level of significance					
freedom	50 %	90 %	95 %	98 %	99 %	99.9 %
3	0.77	2.35	3.18	4.54	5.84	12.94

Obviously, we can interpret that classified worth of 't' is considerably more raised than critical worth of it. So, it very well may be reasoned that the friends and relatives between porosity boundary, Forchheimer number, speed power record and nanoparticle volume part with skin rubbing and intensity move rate are past 99.9% substantial.

TABLE 6: VALUES OF SKIN FRICTION AND NUSSELT NUMBER WITH VARIOUS VALUES OF POROSITY PARAMETER (k_1):

	C_f	r	Increment in ethylene glycol than Engine oil	Nur		Increment in ethylene glycol than Engine oil
k_1	Ethylene glycol	Engine oil	$\frac{\left (ii)\right - \left \left(i\right)\right }{\left i\right } \times 100\%$	Ethylene glycol	Ethylene Engine (i)	$\frac{(iv) - (iii)}{(iii)} \times 100\%$
0	-0.8655	-0.8965	3.58	1.4687	2.7003	83.85
0.1	-1.0207	-1.1003	7.80	1.4571	2.6883	84.50
0.2	-1.1617	-1.2629	8.71	1.4462	2.6775	85.13
0.3	-1.2909	-1.4234	10.26	1.4362	2.6675	85.73
0.4	-1.3756	-1.5305	11.26	1.4286	2.6601	86.20

TABLE 7: VALUES OF SKIN FRICTION AND NUSSELT NUMBER WITH VARIOUS VALUES OF FORCHHEIMER NUMBER (k_2):

	C_f	r	Increment in ethylene glycol than Engine oil			Increment in ethylene glycol than Engine oil
k_2	Ethylene glycol	Engine oil	$\frac{\left (ii)\right - \left (i)\right }{\left i\right } \times 100\%$	Ethylene glycol	Engine oil	$\frac{(iv) - (iii)}{(iii)} \times 100\%$
0	-1.1018	1.2522	13.65	1.4513	2.6767	84.43
0.1	-1.0207	- 1.1321	10.91	1.4571	2.6823	84.09
0.2	-0.9329	1.0213	9.48	1.4633	2.6883	83.72
0.3	-0.8364	0.9023	7.88	1.4701	2.695	83.32

0.4	-0.7284	- 0.7734	6.18	1.4778	2.7025	82.88
-----	---------	-------------	------	--------	--------	-------

TABLE 8: VALUES OF SKIN FRICTION AND NUSSELT NUMBER WITH VARIATION OF VELOCITY POWER INDEX (n):

	C_f	r	Increment in ethylene	Nur		Increment in ethylene
n	Ethylene glycol	Engine oil	glycol than Engine oil $\frac{ (ii) - (i) }{ i } \times 100\%$	Ethylene glycol	Engine oil	glycol than Engine oil $\frac{(iv) - (iii)}{(iii)} \times 100\%$
0.1	-0.7457	-0.7865	5.47	1.4777	2.7019	82.85
0.2	-0.9615	1.02233	6.33	1.4645	2.6911	83.76
0.3	-1.1462	-1.2231	6.71	1.4534	2.6824	84.56
0.4	-1.3096	-1.4025	7.09	1.4438	2.6752	85.28
0.5	-1.3851	-1.5056	8.70	1.4394	2.672	85.63

OUTCOMES AND ITS ANALYSIS:

The result of this assessment is arranged here as tables and charts. Then we really try to grasp that result through a scope of perspective. The mathematical information and the diagrams are created by conceding a bunch of appropriate qualities for each variables of the course, for example,

 $\phi = 0.1, M = 0.2, N_r = 0.1, m = 8, P_r = 40.36$ (*Ethylene glycol*)/100 (Engine oil), $C_T = 0.1$. As we can see in tables6-9 that every one of the appropriate boundaries like porosity boundary, Forchheimer steady, speed power record and Nanoparticle volume division significantly affect wall shear pressure and pace of intensity transmission of the current.

TABLE 9: VALUES OF SKIN FRICTION AND NUSSELT NUMBER WITH VARIOUS VALUES OF NANOPARTICLE VOLUME FRACTION (**):

	$C_f r$		Increment in ethylene glycol	Nur		Increment in ethylene glycol
φ	Ethylen e glycol	Engine oil	than Engine oil $\frac{ (ii) - (i) }{ i } \times 100\%$	Ethylen e glycol	Engine oil	than Engine oil $\frac{(iv) - (iii)}{(iii)} \times 100\%$
0.00	-0.8185	-0.8924	9.03	1.7376	3.2767	88.57
0.03	-0.8722	-0.9440	8.23	1.6513	3.0932	87.32
0.06	-0.9315	-1.0050	7.89	1.5669	2.9143	85.99
0.09	-0.9972	-1.0614	6.44	1.4842	2.7396	84.58
0.12	-1.0702	-1.1260	5.21	1.4032	2.5688	83.06

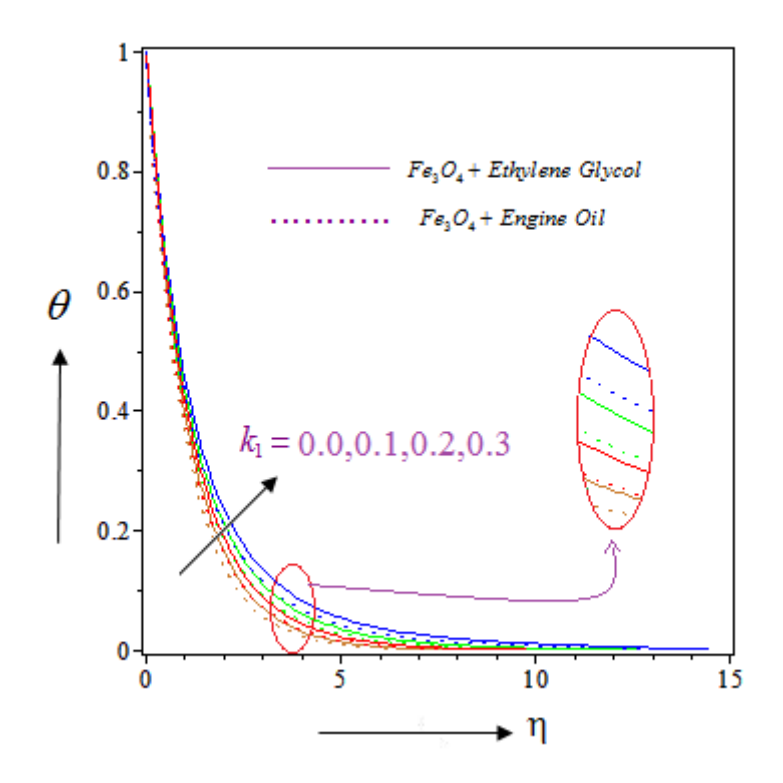


FIGURE 2: EFFECT OF POROSITY PARAMETER (k_1) ON TEMPERATURE OF THE FLOW

INFLUENCE OF POROSITY PARAMETER k_1 :

In table 6 we examine that with the acceleration of porosity boundary the mathematical worth of skin grating coefficient fills in the negative side for both Fe3O4-ethylene glycol and Fe3O4-motor oil nanofluid. This happens on the grounds that when porosity of a medium upsurges, the void hole in the medium ascents and the nanofluid will in general fitting that hole. Thus, the speed of the stream declines and skin grinding from the sheet ascends in esteem. Likewise, we perceive that the distinction in size of skin erosion between two nanofluid ascends with the strengthening in and skin rubbing of Fe3O4motor oil nanofluid is on the higher than Fe3O4-ethylene glycol. Correspondingly, in the event of intensity development of the stream the nuclear power stream diminishes with the increment of for the two liquids. Increase in porosity boundary brings about expanding hole in the stream surface and since liquid is having a tendency to fill that hole it gets adequate opportunity to retain heat from the warmed surface. Be that as it may, the intensity move of the ongoing declines as the stream lessens. Despite the fact that, it is astounding to take note of that the intensity move pace of Fe3O4-motor oil nanofluid is practically 83.85% higher than Fe3O4-ethylene glycol without any and the distinction of Nusselt number between two liquids gets improved up to 86.2% with the higher upsides of. Because of higher warm conductivity of Fe3O4 nanoparticle, it retains the nuclear power from the radiative sheet all the more productively the base liquids. However, because of higher atomic develop Fe3O4 motor oil requires more nuclear power to warm up than ethylene glycol. That is the reason; the pace of nuclear power transmission is higher for Fe3O4-motor oil nanofluid than Fe3O4-ethylene glycol nanofluid. We are endeavoring to see the impact of in the temperature of the stream as exhibited in Fig 2. We found that the temperature of the liquid raised with the impact of porosity boundary and for a proper worth of the temperature profile of the stream lessened with the rising separation from the wall and will in general zero asymptotically. Additionally, the temperature of the Fe3O4-motor oil nanofluid is lesser than Fe3O4-ethylene glycol nanofluid. So from here we can presume that Fe3O4-motor oil nanofluid is more effective to stream nuclear power without expanding the stream temperature, which is a critical nature of an intensity move liquid. In Fig 3 we notice that that higher worth of reduces the speed of the stream

for the two liquids. In any case, Fe3O4-motor oil has higher speed because of lower thickness than Fe3O4-ethylene glycol for each proper worth of.

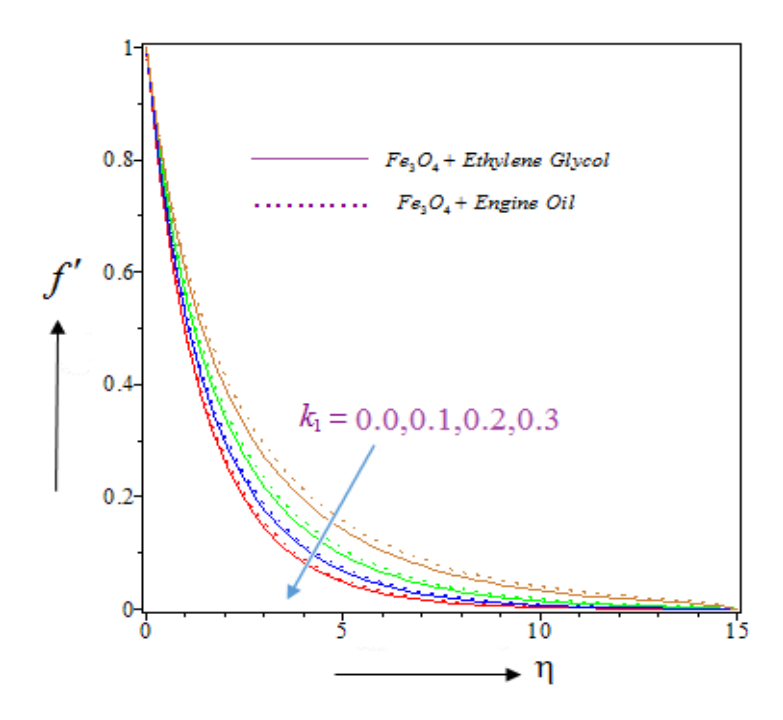


FIGURE 3: EFFECT OF POROSITY PARAMETER (k_1) ON VELOCITY OF THE FLOW

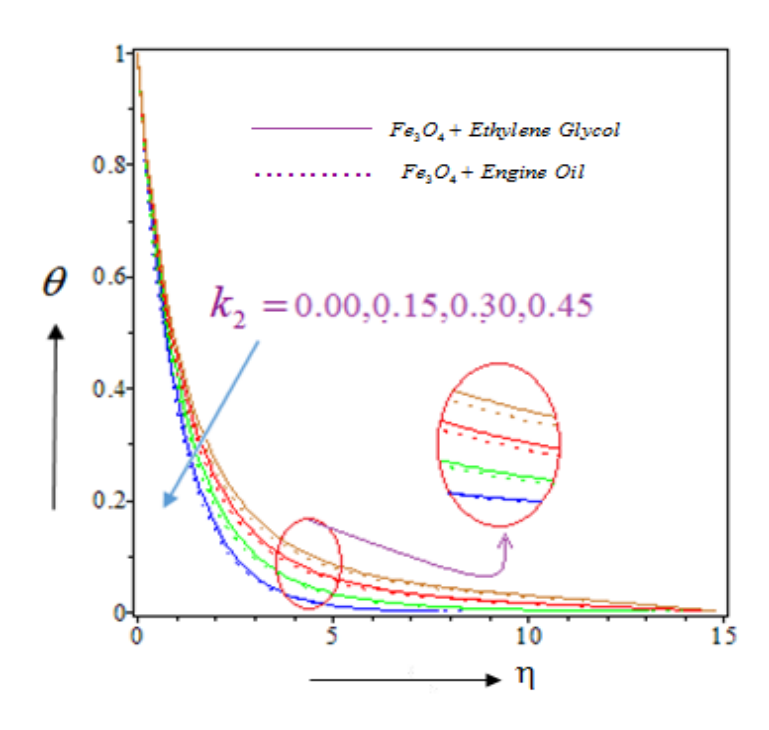


FIGURE 4: EFFECT OF FORCHHEIMER NUMBER (k_{2}) ON TEMPERATURE OF THE FLOW

INFLUENCE OF FORCHHEIMER NUMBER k_2 :

In Table 7 we examine the end result of Forchheimer number on the skin grating and decreased Nusselt number of the stream. We witness that skin grinding decreases and Nusselt number enhances with the

impact in Forchheimer number. Likewise, we distinguish that the distinction in the Nusselt number between two nanofluids reduces from 84.43% to 82.8 % with rising worth of. This suggests that with the ascent of the intensity move rate increment more rapidly for Fe3O4-ethylene glycol liquid than Fe3O4-motor oil liquid. On the opposite side same impact is seen in the event of skin grating coefficient. We see that the drag force is more in greatness for motor oil base liquid than Fe3O4-ethylene glycol liquid. With the acceleration in the drag force diminishes however the diminishing rate is a lot higher for Fe3O4-ethylene glycol liquid. The impact of on the temperature and speed of the current is portrayed in Figs. 4, 5. We see that the thickness of warm limit layer of both of the stream diminishes with expansion in. Additionally, when Forchheimer number expansions in the stream, the distinctions of the liquid temperature decreased as seen in Fig 4. In Fig 5 we saw that Forchheimer number affects the contrast between the speeds of both the liquids. However, for expanding in leads lower drag force between the surface and fluids and subsequently the speeds of the two liquids are on the higher side.

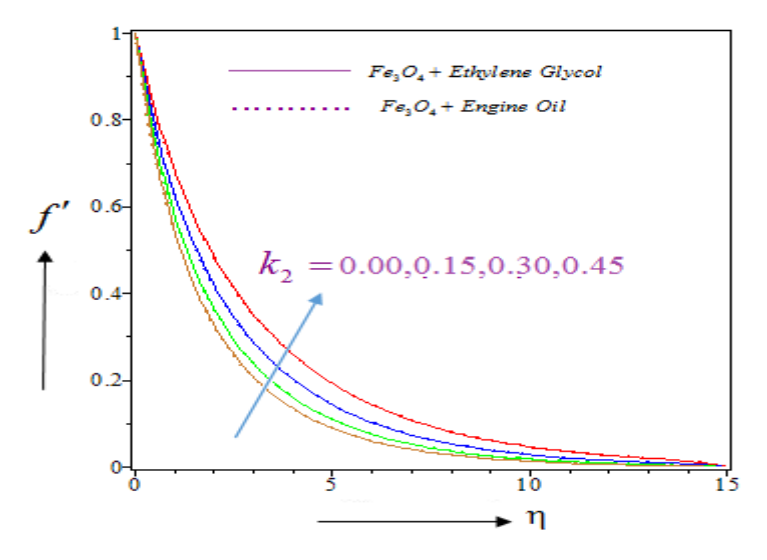


FIGURE 5: EFFECT OF FORCHHEIMER NUMBER (k_2) ON VELOCITY OF THE FLOW

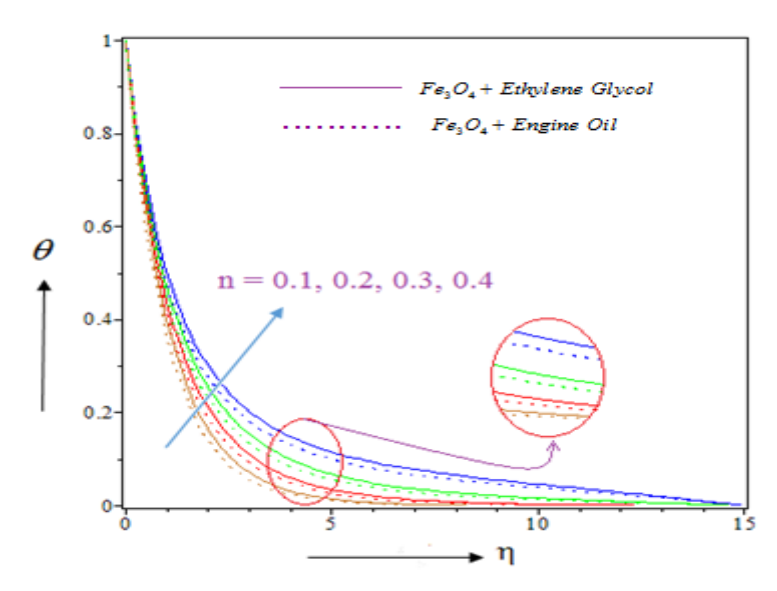


FIGURE 6: EFFECT OF VELOCITY POWER INDEX (N) ON TEMPERATURE OF THE FLOW

INFLUENCE OF VELOCITY POWER INDEX:

It is seen in table 8that with upgrade in results higher drag force among strong extending wall and fluid streaming on the sheet. Likewise in the event of ethylene glycol the drag force is 5.47% not as much as motor oil when speed power file is viewed as the worth 0.1 and when the power record is taken to the worth 0.5 the distinction become 8.7%. This implies that when power record raises the distinction additionally increments. Comparative pattern is seen in the event of intensity move rate for both the liquids. At first for the distinction of intensity move rate is 82.85% and when it arrives at the worth the distinction becomes 85.63%. Subsequently we can get to the place that higher speed power list upgrades the intensity move limit of nanofluids yet for motor oil base liquid it increments at a lot higher rate than Fe3O4-ethylene glycol liquid. As it is recognized in Fig 6, that the temperature of the two liquids is diminished steadily with the expansion in range from the extending wall and will in general zero asymptotically for a proper worth of. Likewise, for each nanofluid, current temperature is by all accounts corresponding with yet the temperature of the Fe3O4-ethylene glycol nanofluid is higher than the other in all cases. In Fig 7 we look at that speed power record heightens the speed and the motor energy of the stream. Additionally, the distinction of speed between two liquids is insignificant at n=0.1 however the distinction develops with higher worth of and when spans to 0.5 speed of the Fe3O4-motor oil nanofluid surpasses Fe3O4-ethylene glycol nanofluid.

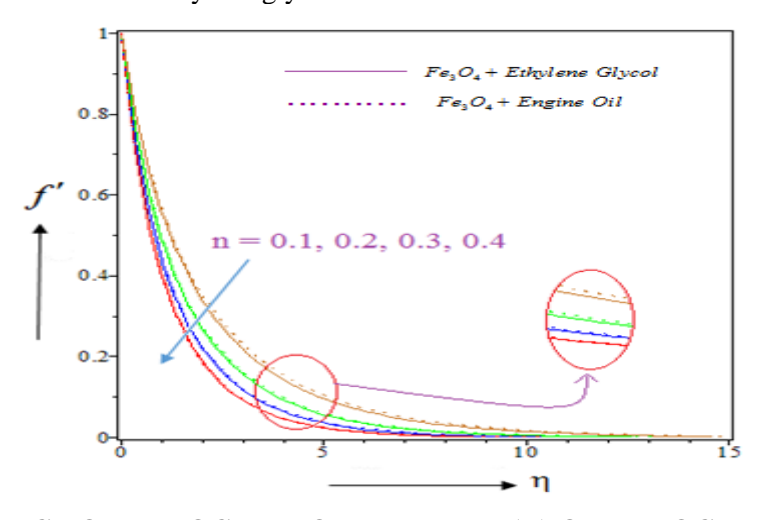


FIGURE 7: EFFECT OF VELOCITY POWER INDEX (N) ON VELOCITY OF THE FLOW

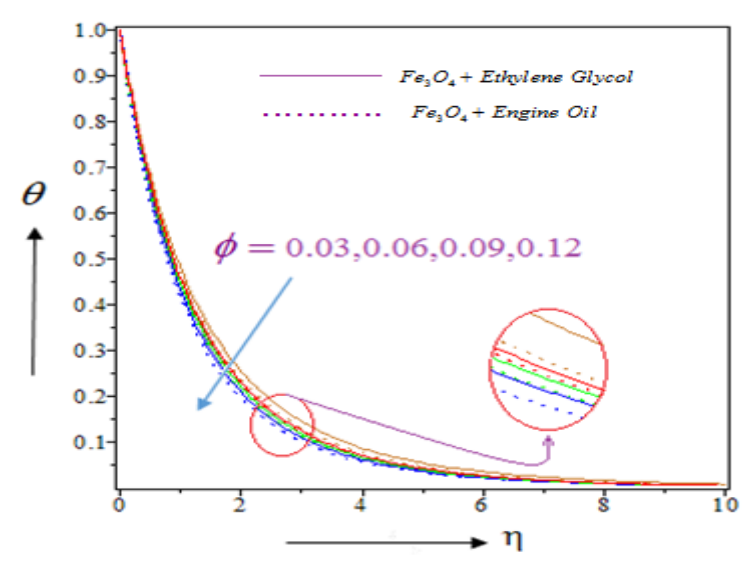


FIGURE 8: EFFECT OF NANOPARTICLE VOLUME FRACTION (ϕ) ON TEMPERATURE OF THE FLOW

INFLUENCE OF NANOPARTICLE VOLUME FRACTION:

Assuming we expand some nanoparticle in the base liquid we witness that the retard force among wall and liquid improves as uncovered in table 9. We see that with higher nanoparticle volume division in the base fluid because of the retard contact among particles and liquid the skin erosion becomes more prominent. On the opposite side, skin erosion of Fe3O4-motor oil nanofluid is higher than Fe3O4ethylene glycol liquid. The distinction of drag force between two liquids is 9.03% when there is no nanoparticle in the fluid and the distinction gets brought down to 5.21% when we enlarge nanoparticle in the stream up to 12%. Moreover, same impact is uncovered for the intensity move of the stream. With the more noteworthy worth of presence of Fe3O4 nanoparticle in the stream reduce the intensity move pace of the stream in light of the fact that because of the presence of nanoparticle the stream encounters a more noteworthy drag force from the wall. So, the speed of the current gets slower as seen in table 9 and subsequently the intensity move rate reduces. Again, for higher Prandtl number motor oil can move 88.57% more nuclear power than ethylene glycol in presence of Fe3O4 nanoparticle. However, the presence of the nanoparticle in the framework up to 12% brought down the hole of intensity move rate down to 83.06%. If we dissect Fig 8 we see that with the higher level of nanoparticle in the stream decline the temperature of the framework. Again, for more intricate atomic design of motor oil than ethylene glycol, the temperature increase of the Fe3O4-motor oil liquid framework is on the slower side. Yet, more presence of nanoparticle declines the temperature hole between two liquids as the presence of Fe3O4 nanoparticle takes the errand to retain the nuclear power in general happy than base liquids. Again, the speed of the stream slowly diminishes since the drag force increment with the expanded the level of nanoparticle as distinguished in Fig. 9. At first close to the wall the impact of the presence of nanofluid isn't seen at large but at some separation from the wall for example (approx.) a minor impact is seen and the speed of the current gets brought down with higher level of presence of nanoparticle in the stream.

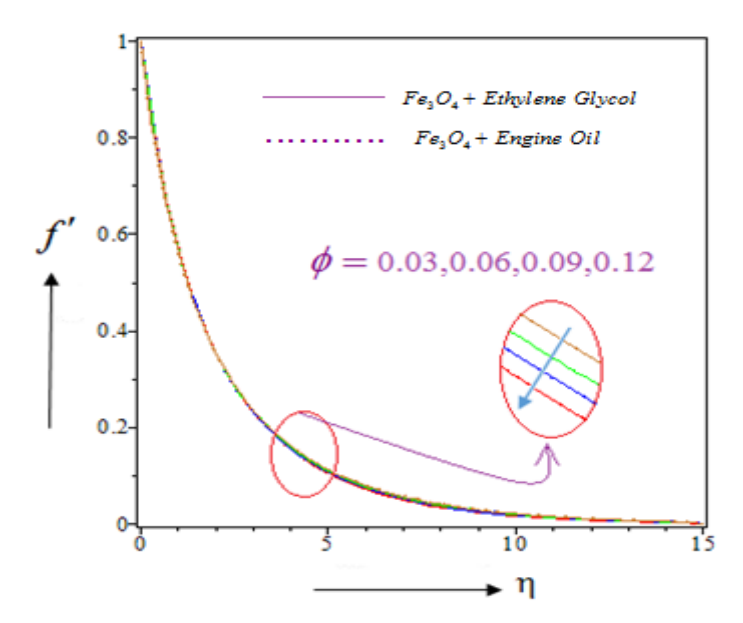


FIGURE 9: EFFECT OF NANOPARTICLE VOLUME FRACTION (ϕ) ON VELOCITY OF THE FLOW

INFERENCE OF THE PRESENT WORK:

In this examination we investigate a set-up of halfway differential conditions accomplished from the investigation of MHD limit layer stream of Fe3O4-ethylene glycol and Fe3O4-motor oil nanofluid unmistakably prompted by uninterruptedly expanding surface in a non - Darcy permeable medium. Subsequent to disentangling the scientific and mathematical arrangements of the model we examine the intensity move execution, the variety in skin grinding coefficient, the temperature and speed of the liquid framework through legitimate diagrams and charts. We additionally explore the legitimacy of the connection between the appropriate elements of the stream and the above quantifiable properties of the

stream by relationship coefficients and Fisher's t-test. Toward the finish of all the challenging examination we have come to the succeeding derivation:

- Due to higher Prandtl number, Fe3O4-motor oil can convey considerably more nuclear power than Fe3O4-ethylene glycol and the thing that matters is around 88.57% to 82.85%. Additionally for complex atomic design than ethylene glycol, motor oil, despite the fact that convey more nuclear power, the temperature of Fe3O4-motor oil liquid doesn't ascend more than Fe3O4-ethylene glycol liquid. This result makes Fe3O4-motor oil an effective conveyance vehicle of nuclear power.
- The nuclear power stream has all the earmarks of being diminished by upgrade in porosity factor, Speed regulation file of the stream surface.
- The prevent force among wall and fluids overstates with expanded porosity element of the medium and inverse impact on the current is seen in the event of Forchheimer number.

The results of the ongoing overview qualify motor oil as productive intensity move liquid than ethylene glycol with Fe3O4 nanoparticle. Various businesses like oil industry, rocket designing, ground water designing could be helpful Fe3O4-motor oil liquid as effective coolant liquid and strengthens the creation.

REFERENCES

- [1] Cheng,P., Minkowycz,W.J.: Free convection about a vertical at plate embedded in a porous medium with application to heat transfer from a disk, Jour. Geophys Res 82, 2040-2044 (1977).
- [2] Hong, J.T., Yamada, Y., Tien, C.L.: Effects of non-Darcian and non-uniform porosity on vertical plate natural convection in a porous media, Trans. ASME Jour. Heat Transfer. 109, 356-362 (1987).
- [3] Lai,F.C., Kulacki, F.A.: Non-Darcy mixed convection along a vertical wall in a saturated porous medium, Int. Jour. Heat Mass Transf. 113, 252-255 (1991).
- [4] R. Kandasamy, I. Muhaimin, A. K. Rosmila, The performance evaluation of unsteady MHD non-Darcy incompressible copper nanofluid flow over a porous wedge due to renewable (solar) energy, Renewable Energy. 64, 1-9 (2014).
- [5] M.Lebeau, J. M. Konrad, Non-Darcy flow and thermal radiation in convective embankment modeling, Comp. and Geotech. 73, 91-99(2016).
- [6] L. J.Crane, Flow past a stretching plate, Z. Angew. Maths. Phys. 21 (1970) 645–647.
- [7] C. K. Chen, M. I. Char, Heat transfer of a continuous stretching surface with suction or blowing, J. Math. Anal. Appl. 135 (1988) 568–580.
- [8] G. C. Layek, S.Mukhopadhyay, S. K.Samad, Heat and mass transfer analysis for boundary layer stagnation point flow towards a heated porous stretching sheet with heat absorption/generation and suction/ blowing. IntCommun Heat Mass Transfer, 34 (2007) 347–56.
- [9]A. Ishak, R.Nazar, I. Pop, MHD boundary layer flow due to a moving extensible surface, Jour. Eng. Math. 62; 2008, 23-33.
- [10] P. D.Weidman, E.Magyari, Generalized Crane flow induced by continuous surfaces stretching witharbitrary velocities, ActaMechanica, 209 (2009) 353–362.
- [11] R. Ahmed, M. Mustafa, T. Hayat, A. Alsaedi, Numerical study of MHD nanofluid flow and heat transfer past a bidirectional exponentially stretching sheet, Jour. of Mag. and Mag. Mat.,407, 2016, 69–74.
- [12] M. T. Sk, K. Das, P. K. Kundu, Effect of magnetic field on slip flow of nanofluid induced by a non-linear permeable stretching surface, ApplThermEng104 (2016) 758–766.
- [13] J.K. Zhou, Differential transformation and its application for electrical circuits, Huarjung University Press, Wuuhahn, China, 1986 (in Chinese).
- [14] M.J. Jang, C.L. Chen, Y.C. Liy, Two-dimensional differential transform for Partial differential equations, Appl. Math. Comput. 121(2001) 261–270.
- [15] I. H. A. Hassan, Comparison differential transformation technique with Adomian decomposition method for linear and nonlinear initial value problems Chaos, Solitions and Fractals 36 (2008) 53-65.
- [16] F. Kangalgil, F. Ayaz, Solitary wave solutions for the KdV and mKdV equations by differential transform method, Chaos, solitons and Fractals, 1 (2009) 464-472.

- [17] H. A. Peker, O. Karaoğlu and G. Oturanç: The Differential Transformation Method and Pade approximant for a form of Blasius equation, math and comp app, 2011, 16(2), 507-513.
- [18] B. Kundu, R. Das, K. S. Lee, Differential Transform Method for thermal analysis of exponential fins under sensible and latent heat transfer, Procedia Eng., 2015, 127, 287-294.
- [19] F. Selimefendigil, H. F. Oztop and K. Al-Saleem, Effect of a rotating cylinder in forced convection of ferrofluid over a backward facing step, Int. J. Heat Mass Transf. 372 (2014) 122 133.
- [20] C. E. Nanjundappa, I. S. Shivakumara and M. M. Ravisha, The onset of ferroconvection in a horizontal ferrofluid saturated porous layer heated from below and cooled from above with constant heat flux subject to MFD viscosity, Int. Commun. Heat Mass Transf. 37 (2010) 1246 -1250.
- [21] M. Sheikholeslami and M. Gorji-Bandpy, Free convection of ferrofluid in a cavity heated from below in the presence of an external magnetic field, Powder Technol. 256 (2014) 490 498.
- [22] L. S. R. Titus and A. Abraham, Heat transfer in ferrofluid flow over a stretching sheet with radiation, Int. J. Eng. Research Tech. 3 (2014) 2198 2203.
- [23] M. Sheikholeslami and D. D. Ganji, Ferrohydrodynamic and magnetohydrodynamic effects on ferrofluid flow and convective heat transfer, Energy 75 (2014) 400 410.
- [24] P. Ram and K. Sharma, Revolving ferrofluid flow under the influence of MFD viscosity and porosity with rotating disk, J. Electromagnetic Analysis Appl. 3 (2011) 378 386.
- [25] S. A. Shehzad, Z. Abdullah, A. Alsaedi, F. M. Abbasi and T. Hayat, Thermally radiative three-dimensional flow of Jeffrey nanofluid with internal heat generation and magnetic field, J. Magn. Magn. Mater. 397 (2016) 108 114.
- [26] T. Hayat, M. Imtiaz and A. Alsaedi, Impact of magnetohydrodynamics in bidirectional flow of nanofluid subject to second order slip velocity and homogeneous–heterogeneous reactions, J. Magn. Mater. 395 (2015) 294 302.
- [27] A. Gul, I. Khan, S. Shafie, A. Khalid and A. Khan, Heat transfer in MHD mixed convection flow of a ferrofluid along a vertical channel, Plos One 10 (11) (2015) e0141213.
- [28] T. Hayat, M. Imtiaz, A. Alsaedi and F. Alzahrani, Effects of homogeneous-heterogeneous reactions in flow of magnetite- Fe₃O₄ nanoparticles by a rotating disk, J. Mol. Liq. 216 (2016) 845 855.
- [29] X. Li, F. Zhong, X. Fan, X. Huai, J. Cai, Study of turbulent heat transfer of aviation kerosene flows in a curved pipe at supercritical pressure, Applied Thermal Engineering 30 (2010) 1845-1851.
- [30] D. K. Agarwal, A. Vaidyanathan, S. S. Kumar, Investigation on convective heat transfer behaviour of kerosene-Al2O3 nanofluid, Applied Thermal Engineering 84 (2015), 64-73.
- [31] D. K. Agarwal, A. Vaidyanathan, S. S. Kumar, Experimental investigation on thermal performance of kerosene–graphene nanofluid, Experimental Thermal and Fluid Science 71 (2016) 126–137.
- [32] U. Khan, N. Ahmed, M. Asadullah, S. T. Mohyud-din, Effects of viscous dissipation and slip velocity on two-dimensional and axisymmetric squeezing flow of Cu-water and Cu-kerosene nanofluids, Propulsion and Power Research 2015 4(1) 40–49.
- [33] Rahman M. ATM., Alam M.S., Choudhury M. K., Thermophoresis particle deposition on unsteady two-dimensional forced convective heat and mass transfer flow along a wedge with variable viscosity and variable Prandtl number: Inter. Comm. in Heat and Mass Transf, 39(4),2012, 541-550.